Factors Controlling the Formation of Core−Shell Zeolite−Zeolite Composites

Younes Bouizi,[†] Loïc Rouleau,[‡] and Valentin P. Valtchev*[,†]

Laboratoire de Matériaux à Porosité Contrôlée, UMR-7016 CNRS, ENSCMu, Université de Haute Alsace, 3, rue Alfred Werner, 68093 Mulhouse Cedex, France, and Institut Français du Pétrole, BP3 - 69390 Vernaison, France

Received May 18, 2006. Revised Manuscript Received July 17, 2006

Core−shell zeolite−zeolite composites possessing single-crystal cores and polycrystalline shells of different zeolite structure types were synthesized. The formation of an intergrown shell structure was induced by preliminary seeding of the core crystals and subsequent secondary growth under hydrothermal conditions. The utilization of seeds suppressed the influence of framework particularities of the core crystals on the formation of the shell layer. Hence, the couples of zeolitic materials were chosen in a way to reveal the effect of differences between the chemical compositions and crystallization conditions of core and shell zeolites on the formation of the desired composite. The following couples of microporous materials were involved in the investigation: SOD-LTA, BEA-LTA, FAU-MFI, MFI-BEA, and MFI-MFI (ZSM-5−silicalite-1), the first structure type representing the core and the second the shell material. Complementary techniques, such as XRD, TG/DTA, SEM/TEM, EDS, and X-ray fluorescence analyses, were employed to fully characterize the composites and their intermediates. The integrity of the shell layer was tested by N_2 adsorption measurements on materials comprising calcined core crystals and noncalcined organic template-containing shells thus providing information about the percentage of composites possessing defect-free shells. The results showed the paramount importance of chemical compatibility between shell and core crystals for the successful formation of a core−shell structure. The shell growth was also determined by the match of the crystallization fields of the core and shell materials, that is, at least partial overlapping was required to form a core−shell composite.

Introduction

The preparation of hollow inorganic microcapsules possessing a tiny shell and a relatively large core space enabling the storage of various species has attracted considerable attention.[1] Special attention has been paid to inorganic shells because of their relatively high thermal, mechanical, and chemical stability. Thus, various oxides and sulfides have been prepared in the form of microcapsules, namely, with spherical geometry.[2] This original class of materials offers certain advantages in the development of optical, sensing, semiconducting, and low weight materials. Further, such microcapsules might be employed for storage and controlled drug release or as catalytic microreactors. The latter applications require shells with controlled porosity; consequently, the preparation of microcapsules built up of microporous or mesoporous materials with well-defined pore systems is highly desired. Thus, mesoporous microcapsules made of aluminosilicates,[3a] titanosilicates,[3b] manganese oxide,[3c] and carbon[3d] have been prepared. Microporous zeolite microcapsules have also been synthesized using polystyrene spheres as sacrificial templates and applying layer-by-layer[4] or secondary growth[5] synthesis approaches. Tang and co-workers[6] developed an original procedure, where sacrificial templating mesoporous spheres were employed. After seeding, the spheres were subjected to vapor phase transport synthesis. During the growth of a zeolite shell, the mesoporous silica was consumed, thus leaving a hollow zeolite replica of the templating mesoporous material. This approach enables an easy encap-

* Author to whom correspondence should be addressed. E-mail: V.Valtchev@uha.fr.

[†] Université de Haute Alsace.

[‡] Institut Français du Pétrole.

(1) Caruso, F. In *Engineering of Core - shell Particles and Hollow Capsules in Nanosurface Chemistry;* Rosoff, M., Ed.; Marcel Dekker: New York, 2001; pp 505−525.

(2) (a) Imhof, A.; Pine, D. J. *Nature* **1997**, *389*, 948. (b) Holland, B. T.; Blanford, C. F.; Stein, A. *Science* **1998**, *281*, 538. (c) Wijnhoven, J.; Vos, W. L. *Science* **1998**, *281*, 802. (d) Wang, X. D.; Yang, W. L.; Tang, Y.; Wang, Y. J.; Fu, S. K.; Gao, Z. *Chem. Commun.* **2000**, 2161. (e) Caruso, F.; Shi, X. Y.; Caruso, R.; Susha., A. *Adv. Mater.* **2001**, *13*, 740. (f) Meyer, U.; Larsson, A.; Hentze, H. P.; Caruso, R. A. *Adv. Mater.* **2002**, *14*, 1768. (g) Yoon, S. B.; Sohn, K.; Kim, J. Y.; Shin, C. H.; Yu, J. S.; Hyeon, T. *Adv. Mater.* **2002**, *14*, 19. (h) Kamata, K.; Lu, Y.; Xia, Y. N. *J. Am. Chem. Soc.* **2003**, *125*, 2348. (i) Bao, J. C.; Liang, Y. Y.; Xu, Z.; Si, L. *Adv. Mater.* **2003**, *15*, 1832. (j) Shao, M. W.; Wang, D. B.; Hu, B.; Yu, G. H.; Qian, Y. T. *J. Cryst. Growth* **2003**, *249*, 549. (k) Hu, Y.; Chen, J. F.; Chen, W. M.; Li, X. L. *Adv. Funct. Mater.* **2004**, *14*, 383. (l) Li, X. L.; Lou, T. J.; Sun, X. M.; Li, Y. D. *Inorg. Chem.* **2004**, *43*, 5442. (m) Wang, Y. L.; Cai, L.; Xia, Y. N. *Adv. Mater.* **2005**, *17*, 473. (n) Ren, N.; Wang, B.; Yang, Y. H.; Zhang, Y.-H.; Yang, W.-L.; Yue, Y.-H.; Gao, Z.; Tang, Y. *Chem. Mater.* **2005**, *17*, 2582.

(3) (a) Li, Y.; Shi, J.; Hua, Z.; Chen, H.; Ruan, M.; Yan, D. *Nano Lett.* **2003**, *3*, 609. (b) Li, W.; Coppens, M.-O. *Chem. Mater.* **2005**, *17*, 2241. (c) Yuan, J.; Laubernds, K.; Zhang, Q.; Suib, S. L. *J. Am. Chem. Soc.* **2003**, *125*, 4966. (d) Xia, Y.; Mokaya, R. *Adv. Mater.* **2004**, *16*, 886.

(4) (a) Wang, X. D.; Yang, W. L.; Tang, Y.; Wang, Y. J.; Fu, S. K.; Gao, Z. *Chem. Commun.* **2000**, 2832. (b) Valtchev, V.; Mintova, S. *Microporous Mesoporous Mater.* **2001**, *43*, 41.

(5) (a) Valtchev, V. *Chem. Mater.* **2002**, *14*, 956. (b) Valtchev, V. *Chem. Mater.* **2002**, *14*, 4371.

(6) Dong, A.; Wang, Y.; Tang, Y. Ren, N.; Zhang, Y.; Gao, Z. *Chem. Mater.* **2002**, *14*, 3217.

10.1021/cm0611744 CCC: $33.50
Published on Web 09/07/2006

sulation of catalytically active metals deposited on the inner part of the shell.[7] The same group reported the preparation of zeolite microcapsules by using $CaCO_3$ and $Fe_3(SO_4)_2 \cdot 2H_2O$ cores that later were eliminated using wet chemistry methods.[8] However, substantial disadvantages of hollow microcapsules are the low mechanical strength and the absence of any functionality of the empty core structure. Core−shell structures, where the access to a large core with specific properties is controlled by a tiny shell, with different functionalities would increase considerably the areas of application of such materials. In addition, core−shell materials are expected to show much higher mechanical stability with respect to hollow microcapsules. Such a core−shell material, possessing a core and a shell of different porosities, was reported by Yu et al.[9] The material comprised a zeolite core and a mesoporous shell and was further employed in the preparation of hollow mesoporous carbon microcapsules. The formation of carbon microcapsules was because the carbon is difficult to be infiltrated in zeolite micropores. Consequently, during the dissolution of the inorganic template, only the carbon replicating the mesopore shell remains.

For catalytic and separation purposes, a material combining a microporous shell that could control the access to a microporous or mesoporous core would be much more interesting. For instance, zeolite−zeolite microcomposites might be used for the simultaneous separation and storage of small molecules. Separation by the shell structure and further catalytic transformation in the core might also be performed on such microcomposites. Very recently, the preparation of core−shell zeolite−zeolite composites possessing core and shell of different structural types was reported.[10] This is the first case of complete overgrowth of a zeolite by another, although several examples of intergrowth or partial overgrowth of two different zeolite types have been published in the past. The latter phenomena are because several zeolitic materials possess similar building units but with different spatial arrangements.[11] Under specific synthesis conditions, the cocrystallization of such materials may lead to intimate intergrowth between the two structures. A classical example is the microporous material obtained by the polytypical intergrowth of ERI- and OFF-type framework topologies.[12] Polytypical intergrowth was also reported for the couples MFI-MEL[13] and MAZ-MOR.[14] Nanofibers formed by an epitaxial growth of zeolite Beta on SSZ-31 was reported by Nair et al.[15] Also, several high-silica zeolitic materials result from the intergrowth of two or more polymorphs, like zeolite Beta,[16] ZSM-48,[17] and so forth.[11] For the preparation of core−shell zeolite structures, the epitaxial overgrowth is more important as a crystallization phenomenon. Such a kind of overgrowth of cancrinite on large sodalite crystals was reported by Okubo et al.[18] Epitaxial growth of zeolite A on large zeolite X (FAU-type) crystals synthesized by a modified Charnell's method was also published[19a] as well as the growth of zeolite X on zeolite A cubic face.[19b] A similar type of overgrowth was described by Goossens et al.[20] for the cubic and hexagonal counterparts of the large pore FAU-EMT family. A zeolite film with heteroepitaxial growth of CHA-type material on sodalite (SOD) was described by Wakihara et al.[21] The heteroepitaxial overgrowth of ETS-4 on ETS-10 molecular sieves was used by Tsapatsis and co-workers[22] to prepare oriented molecular sieve membranes. Therefore, the heteroepitaxial could be employed for the modification of the properties of many zeolites. This type of overgrowth, however, takes place on a specific crystal face and thus cannot be employed for the preparation of core−shell zeolite−zeolite composites possessing single-crystal cores.

The preliminary adsorption of nanoseeds on the core crystals and their further secondary growth allowing the formation of core−shell materials was exemplified by the preparation of BEA-MFI[10a] and mordenite−silicalite-1[10b] core−shell structures. These investigations proved the feasibility of the seeding approach in the preparation of core−shell materials without providing, however, the limits of the method. As known, the zeolites are metastable compounds that may easily be transformed into other porous or nonporous materials under hydrothermal conditions. The goal of the present study was to determine the factors controlling the formation of core−shell zeolite−zeolite composites by using seeding crystals that induce the growth of the zeolite shell. A series of zeolitic materials were employed so as to investigate the effect of framework composition and the synthesis conditions of the core and shell crystals on the formation of microcomposites.

Materials and Methods

Synthesis of Core Crystals. The relatively large single crystals employed as core materials were synthesized according to different

(7) (a) Dong, A.; Wang, Y.; Wang, D.; Yang, W.; Zhang, Y.; Ren, N.; Gao, Z.; Tang, Y. *Microporous Mesoporous Mater.* **2003**, *64*, 69. (b) Dong, A.; Ren, N.; Yang, W.; Wang, Y.; Zhang, Y.; Wang, D.; Hu, J.; Gao, Z.; Tang, Y. *Adv. Funct. Mater.* **2003**, *13*, 943.
(8) Wang, D.; Zhu, G.; Zhang, Y.; Yang, W.; Wu, B.; Tang, Y.; Xie, Z. *New J. Chem.* **2005**, *29*, 272.
(9) Yu, J.-S.; Yoon, S. B.; Lee, Y. J.; Yoon, K. B. *J. Phys. Chem. B* **2005**, *109*, 7040.
(10) (a) Bouizi, Y.; Diaz, I.; Rouleau, L.; Valtchev, V. P. *Adv. Funct. Mater.* **2005**, *15*, 1955. (b) Bouizi, Y.; Rouleau, L.; Valtchev, V. P. *Microporous Mesoporous Mater.* **2006**, *91*, 70.
(11) Baerlocher, Ch.; Meier, W. M.; Olson, D. H. *Atlas of Zeolite Framework Types*, 5th ed.; Elsevier: Amsterdam, 2001.
(12) Lillerud, K. P.; Raeder, J. H. *Zeolites* **1986**, *6*, 474.
(13) (a) Ohsuna, T.; Terasaki, O.; Nakagawa, Y.; Zones, S. I.; Hiraga, K. *J. Phys. Chem.* **1997**, *101*, 9881. (b) Francesconi, M. S.; Lopez, Z. E.; Uzcategui, D.; González, G.; Hernández, J. C.; Uzcátegui, A.; Loaiza, A.; Imbert, F. E. *Catal. Today* **2005**, *107*−*108*, 809. (c) Thomas, J. M.; Millward, G. R. *J. Chem. Soc., Chem. Commun.* **1982**, 1380.
(14) Leonowicz, M. E.; Vaughan, D. E. W. *Nature* **1987**, *329*, 819.
(15) Nair, S.; Villaescusa, L. A.; Camblor, M. A.; Tsapatsis, M. *Chem. Commun.* **1999**, 921.
(16) Higgins, J. B.; LaPierre, R. B.; Schlenker, J. L.; Rohrman, A. C.; Wood, J. D.; Kerr, G. T.; Rohrbaugh, W. J. *Zeolites* **1988**, *8*, 446.
(17) Schlenker, J. L.; Rohrbaugh, W. J.; Chu, P.; Valyocsik, E. W.; Kokotailo, G. T. *Zeolites* **1985**, *5*, 355.
(18) Okubo, T.; Wakihari, T.; Plévert, J.; Nair, S.; Tsapatsis, M.; Ogawa, Y.; Komiyama, H.; Yoshimura, M.; Davis, M. E. *Angew. Chem., Int. Ed.* **2001**, *40*, 1069.
(19) (a) Porcher, F.; Dusausoy, Y.; Souhassou M.; Lacomte, C. *Mineral. Mag.* **2000**, *64*, 1. (b) de Vos Burchart, E.; Jansen, J. C.; van Bekkum, H. *Zeolites* **1989**, *9*, 432.
(20) Goossens, A. M.; Wouters, B. H.; Buschmann, V.; Martens, J. A. *Adv. Mater.* **1999**, *11*, 561.
(21) Wakihara, T.; Yamakita, Sh.; Iezumi, K.; Okubo, T. *J. Am. Chem. Soc.* **2003**, *125*, 12388.
(22) Jeong, H.-K.; Krohn, J.; Sujaoti, K.; Tsapatsis, M. *J. Am. Chem. Soc.* **2002**, *124*, 12966.

Table 1: Initial Systems and Synthesis Conditions Used for the Preparation of Core and Nanosized Seed Crystals

			synthesis	
	zeolite	molar composition	*T* (°C)	duration (days)
nanocrystals	silicalite-1 (MFI)	$4.5(TPA)_2O:25SiO_2:480H_2O:100EtOH$	80	4
	zeolite A (LTA)	$0.3Na_2O:13.8(TMA)_2O:1.8Al_2O_3:11.25SiO_2:752H_2O$	40	10
	zeolite Beta (BEA)	$4.5(TEA)_2O:0.25Al_2O_3:25SiO_2:295H_2O$	80	15
core crystals	zeolite X (FAU)	$4.76Na_2O:2TrEA:1Al_2O_3:3.5SiO_2:454H_2O$	110	2
	ZSM-5 (MFI)	$0.6K_2O:0.25(TPA)_2O:0.2Al_2O_3:1SiO_2:30H_2O$	170	2
	zeolite Beta (BEA)	$0.275(TEA)_2O:0.6HF:1SiO_2:6H_2O$	140	9
	sodalite (SOD)	$1.0SiO_2:0.5TEAF2.0H_2O:8.0$ethylenediamine	170	14

Table 2. Initial Systems and Synthesis Conditions Used in the Secondary Growth of Shell Structures

		synthesis conditions	
core−shell composite	molar composition	*T* (°C)	duration (h)
SOD(Si)[a]/LTA	$6Na_2O:0.55Al_2O_3:1SiO_2:150H_2O$	100	3
BEA(Si)[a]/LTA	A1: $0.3Na_2O:13.8(TMA)_2O:1.8Al_2O_3:11.25SiO_2:752H_2O$	110	48
	A2: $0.3Na_2O:6.90(TMA)_2O:1.8Al_2O_3:11.25SiO_2:752H_2O$	110	48
	A3: $0.3Na_2O:3.75(TMA)_2O:1.8Al_2O_3:11.25SiO_2:752H_2O$	110	48
	A4: $0.3Na_2O:3.45(TMA)_2O:1.8Al_2O_3:11.25SiO_2:752H_2O$	110	48
	A5: $0.6Na_2O:3.45(TMA)_2O:1.8Al_2O_3:11.25SiO_2:752H_2O$	110	14
FAU/MFI(Si)[a]	$1.5(TPA)_2O:25SiO_2:1500H_2O:100EtOH$	140	24
	$1.5(TPA)_2O:25SiO_2:1500H_2O:100EtOH$	170	12
	$1.5(TPA)_2O:25SiO_2:1500H_2O:100EtOH$	200	1
MFI/MFI(Si)[a]	$1.5(TPA)_2O:25SiO_2:1500H_2O:100EtOH$	200	1
MFI/BEA	$4.5(TEA)_2O:0.25Al_2O_3:25SiO_2:295H_2O$	140	72

[a] (Si) means all-silica material.

recipes published in the open literature (Table 1). FAU-type single crystals ranging between 20 and 40 μm were synthesized according to Hamilton et al.[23] using triethanolamine (TrEA, Fluka) as an aluminum-complexing agent. MFI-type (ZSM-5, Si/Al = 14) single crystals of ca. 20 μm were obtained by a laboratory recipe using the following reactants: potassium hydroxide (Fluka, 85%), tetrapropylammonium (TPA) hydroxide (Fluka, 20% in water), aluminum isopropoxide (Aldrich), colloidal silica (Aldrich, Ludox HS-30), and distilled water. All-silica (Si−BEA) 10−20 μm crystals were grown by the method published by Camblor et al.[24] All-silica sodalite (Si−SOD) crystals with a size of about 20 μm were synthesized following the Bibby and Dale[25] procedure in ethylendiamine (EDA)−fluoride medium and employing tetraethylammonium ($TEAF{\cdot}2H_2O$, Fluka) as a structure-directing agent. All synthesized materials were thoroughly washed with distilled water and were dried at 80 °C overnight. The combustion of the organic structure-directing agent was performed at 600 °C for 6 h in an air atmosphere.

Synthesis of Nanocrystals. The initial systems and synthesis conditions used for the preparation of zeolite nanocrystals further employed as seeds are summarized in Table 1. After synthesis, the zeolite suspensions were purified by four series of high-speed centrifugation (20 000 rpm, 1 h), decanting, and redispersion in distilled water. The pH of the resultant suspensions was adjusted to 9.5 by using 0.1 M NH_3. The zeolite content in the seeding suspensions was about 3 wt %.

Synthesis of Core−Shell Microcomposites. The negative surface charge of the large core crystals was reversed using a 0.5 wt % aqueous solution of a polycation agent (poly(diallyldimethylammonium chloride), Aldrich), and then, the negatively charged nanoseeds were adsorbed. Calcination of the resulting pretreated core crystals at 500 °C for 8 h provided a material with seeds firmly fixed to the surface. The molar compositions and conditions used for the subsequent core−shell composite syntheses are summarized in Table 2.

All secondary growth experiments were performed on calcined core materials. The calcination was necessary to provide seeds firmly stuck to the surface of the support and to liberate the intracrystalline volume of the core materials. The latter was necessary to evaluate the adsorption capacity of the as-synthesized composites and thus the integrity of the shell. A reference experiment without calcination of the core material was performed for each couple. These experiments did not show substantially different stability of the core zeolites upon hydrothermal treatment.

Characterization. The obtained core−shell materials were studied by X-ray diffraction (XRD) using a STOE STADI-P diffractometer in Debye−Scherrer geometry equipped with a linear position-sensitive detector (6° in 2θ) and employing Ge monochromated Cu $K\alpha_1$ radiation. Electron micrographs were taken on a Philips XL30 FEG scanning electron microscope (SEM) equipped with an EDAX energy-dispersive X-ray spectrometer (EDS, Oxford ISIS-Energy). Transmission electron microscopy (TEM) coupled with selected area electron diffraction (SAED) was used to index the crystal faces and to study the interface structure. The TEM images and SAED patterns were taken with a JEOL-4000 EX microscope operating at 400 kV (Cs = 1.0 mm). Nitrogen adsorption measurements were carried out on a Micromeritics ASAP 2010 surface area analyzer. The as-synthesized and calcined samples were analyzed after outgassing at 130 °C and 300 °C, respectively. The elemental analyses of the core crystals were performed on an X-ray fluorescence spectrometer MagiX (Philips). Prior to the analysis, the powdery sample was melted with $Li_2B_4O_7$ at 1300 °C. The resultant glass bead was analyzed under vacuum with a rhodium anticathode (2.4 kW).

Results

The attempts to synthesize core−shell composites without using seeds were not successful, and thus zeolite nanocrystals were used to induce the growth of the shell. In a seeded zeolite film synthesis, the orientation of the layer, at least at the first stages of film formation, is controlled by the seeds.[26] Therefore, a specific effect of the core structure on the shell formation is not likely to be observed. Hence, the couples

(23) Hamilton, K. E.; Coker, E. N.; Sacco, A., Jr.; Dixon, A. G.; Thompson, R. W. *Zeolites* **1993**, *13*, 645.
(24) Camblor, M. A.; Corma, A.; Valencia, S. *Chem. Commun.* **1996**, 2365.
(25) Bibby, D. M.; Dale, M. P. *Nature* **1985**, *317*, 157.

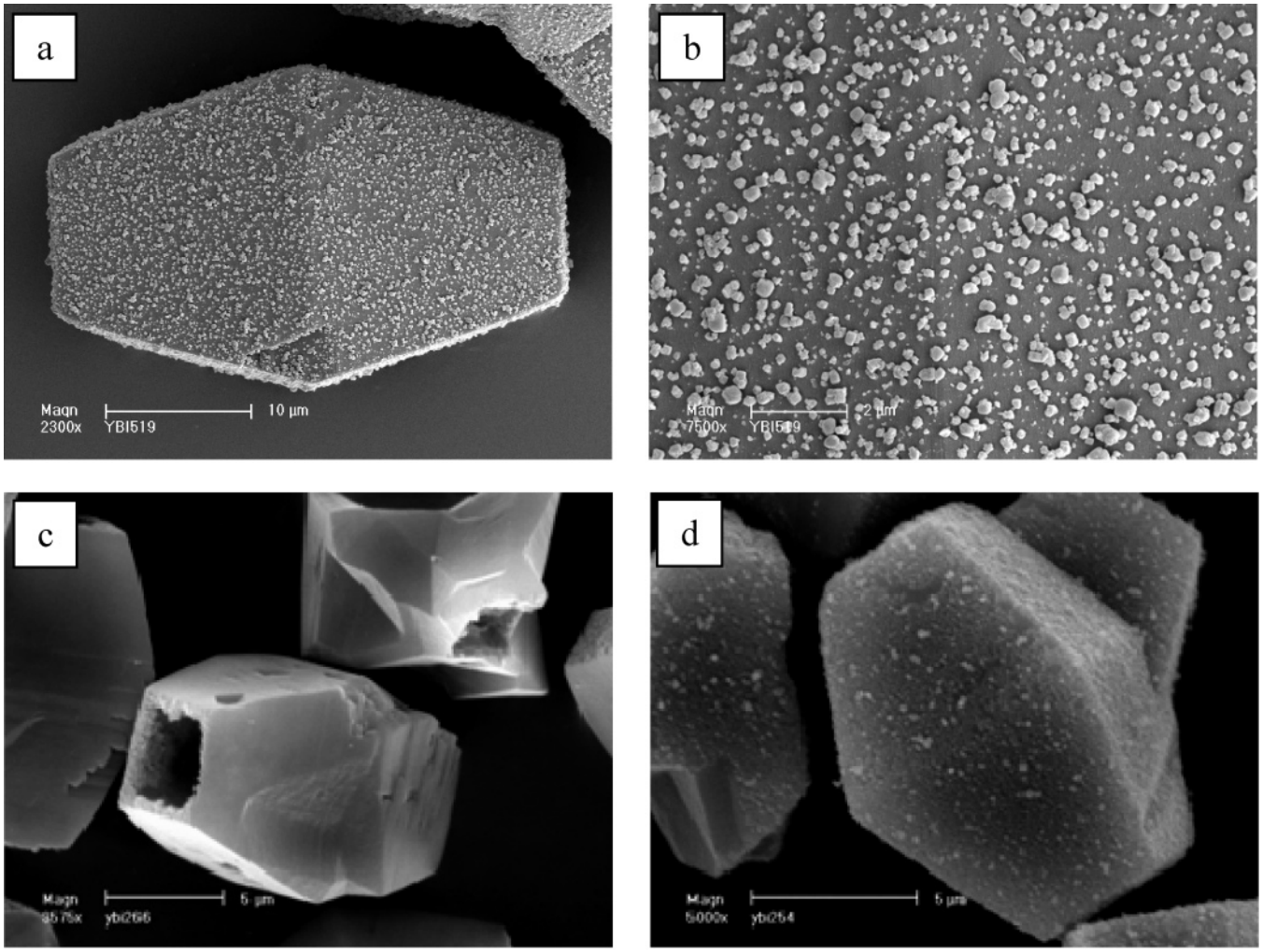

Figure 1. General (a) and close (b) views of a zeolite A−seeded zeolite Beta single crystal. Seeded zeolite Beta crystals subjected to hydrothermal treatment with solutions A2 (c) and A4 (d), respectively.

used in the present study were chosen in a way to reveal the effect of chemical compatibility and the match of crystallization fields of the core and shell materials. The following couples were subjected to investigation:

All-Silica Sodalite (Si−SOD)−Zeolite A (LTA). An all-silica sodalite−zeolite A composite does not present particular interest from a practical point of view. Nevertheless, experiments were performed to study the possibility to grow composites with core and shell with completely different Si/Al ratios. Although a uniform (ca. 70 seeds per 1 μm^2) layer of zeolite A nanoseeds was deposited on the SOD-type core crystals, the formation of a zeolite A shell was not induced. Depending on the synthesis time, partial (for 3 h) or complete (for 6 h) dissolution of the sodalite crystals was observed. This result is obviously due to the substantially different nature of the core and shell materials. Besides totally different compositions of the core and shell structures, the difference in synthesis conditions should be underlined. All-silica sodalite was synthesized at 170 °C, only in the presence of tetraethylammonium, while the secondary growth was performed with a sodium-rich aluminosilicate system at 100 °C. These differences in the crystallization conditions and compositions of core and shell materials are obviously not in favor of the formation of the core−shell structure.

This series of experiments showed also that the use of a gel system for the secondary growth is not convenient for the purposes of the present study. The gel systems yield large amounts of precipitated zeolite material and thus make difficult the separation of the core−shell composites. Therefore, all subsequent syntheses were performed with systems yielding nanocrystals that allow an easy separation of relatively large core−shell composite from the bulk zeolite suspension.

All-Silica Zeolite Beta (Si−BEA)−Zeolite A (LTA). The possibility to combine in a core−shell structure a hydrophobic and a hydrophilic zeolite, respectively, with 12- and 8-membered three-dimensional pore systems, seems very attractive and deserves special attention. However, the first attempts to synthesize Si−BEA−LTA composites were not successful although the LTA-type nanoseeds were relatively homogeneously distributed on the zeolite Beta surface (Figure 1a and b). The core crystals were completely dissolved in the synthesis solution (A1, Table 2), which required the use of more gentle initial solution. A decrease by a factor of 2 of the TMAOH content (A2, Table 2) preserved the core crystals, and the characteristic reflections

(26) Mintova, S.; Hedlund, J.; Valtchev, V.; Schoeman, B. J.; Sterte, J. *J. Mater. Chem.* **1998**, *8*, 2217.

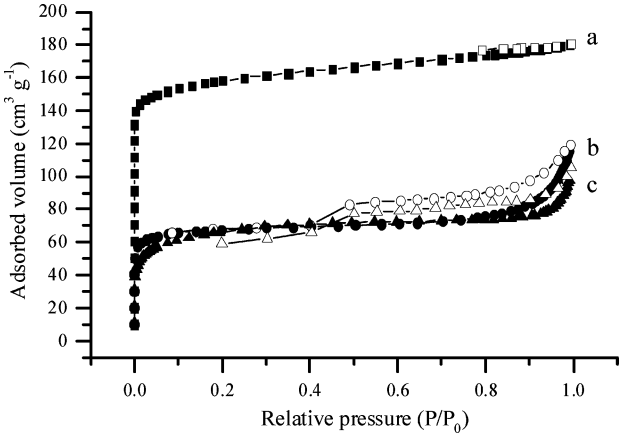

Figure 2. Adsorption−desorption isotherms of the zeolite Beta reference sample and zeolite Beta−zeolite A core−shell composites synthesized with solution A4 (Table 2) for 24 h (b) and 14 h (c).

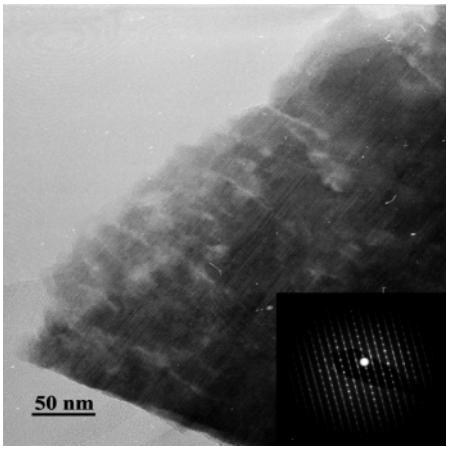

Figure 3. Low-magnification TEM image of a zeolite Beta core crystal nonprotected by a shell, subjected to partial dissolution during the hydrothermal treatment. Inset: Seleted area electron diffraction pattern showing very strong diffusive lines corresponding to the coexistence of polytypes in the zeolite Beta core crystals.

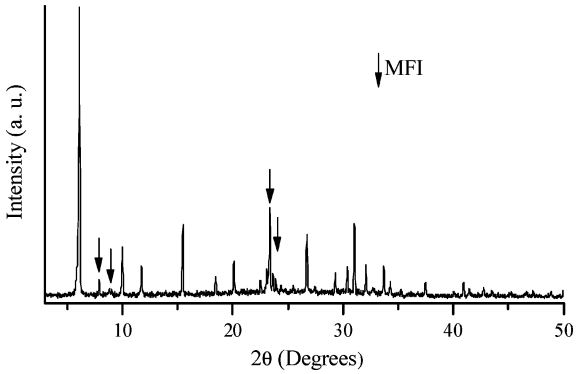

Figure 4. XRD pattern of a zeolite X−silicalite-1 core−shell composite.

of the BEA-type structure were observed in the XRD pattern. The material, however, did not contain peaks that could be attributed to zeolite A. The SEM inspection confirmed that there was no film formation and that holes due to the dissolution of pinacoidal face (00*l*) can be seen on many crystals (Figure 1c). Further decrease of the TMAOH content (A3 and A4, Table 2) allowed the formation of Beta−zeolite A composites according to the XRD analysis. All beta crystals seemed to be covered by a shell, but a closer inspection showed the presence of small areas of uncompleted shells on some crystals (Figure 1d). Neither a second adsorption of seeds followed by hydrothermal treatment nor the increase of the sodium content in the initial solution (A5, Table 2) resulted in a better coverage.

Composites possessing a calcined core and a noncalcined shell were subjected to N_2 adsorption measurements. Adsorption−desorption isotherms of the reference sample (calcined zeolite Beta) and composites synthesized for 14 and 24 h are shown in Figure 2. As can be seen, all isotherms are typical of microporous materials (type I), where the steep uptake at low relative pressure is followed by nearly horizontal adsorption and desorption branches. The composite materials show small hysteresis loops at high relative pressure, which is most probably because of textural porosity formed by stacking of nanoparticles with a narrow particle size distribution. The S_{BET} and micropore volume of the reference material are characteristic of a highly crystalline BEA-type material. As could be expected, these values are lower for the composite materials with respect to the zeolite Beta reference sample. The SEM/TEM investigation revealed that the decrease in the specific surface area was most probably because of the dissolution of core material. SEM analysis showed a very large number of partially covered crystals, which according to the TEM study were subjected to surface dissolution (Figure 3). Besides the surface dissolution, veins reaching deep in the core of large zeolite Beta crystals were observed.

Zeolite X (FAU)−Silicalite-1 (MFI). As stated above, the possibility to combine core and shell of different hydrophobicity and pore system is of interest. Taking into account the differences in the crystallization fields of zeolite X and silicalite-1, different combinations of synthesis temperature and crystallization time were used to find the optimum conditions (Table 2). The XRD analysis of the separated large zeolite X crystals showed the presence of MFI-type materials (Figure 4), and the SEM study confirmed the presence of a layer of nanocrystals on the surface of FAU-type material. However, none of the obtained composites possessed a completed layer. Similarly to the previous couple (BEA-LTA), traces of dissolution were observed on some of the core crystals. Therefore, outside of the crystallization field of a given zeolite, the formation of an accomplished shell is difficult. We anticipate that the low hydrothermal stability of FAU-type material is the reason for the unsuccessful formation of a zeolite X−silicalite-1 composite. In other words, zeolite X dissolves easily outside its crystallization field. We anticipate that because of the dissolution, the chemical equilibrium at the interface between core material and synthesis solution is perturbed, and thus the conditions required for the crystallization of a silicalite-1 shell could not be reached. The dissolution of zeolite X provides Na- and Al-rich species that beyond given limits seem to inhibit the formation of TPA-containing MFI-type materials. The lowest Si/Al ratio of TPA grown MFI-type materials in the absence of alkali cations is about 25.

ZSM-5 (MFI)−Silicalite-1 (MFI). The formation of an all-silica shell (silicalite-1) around a ZSM-5 (Si/Al = 14) crystal is expected to have a positive effect on the catalytic selectivity of the resulting material by blocking the active

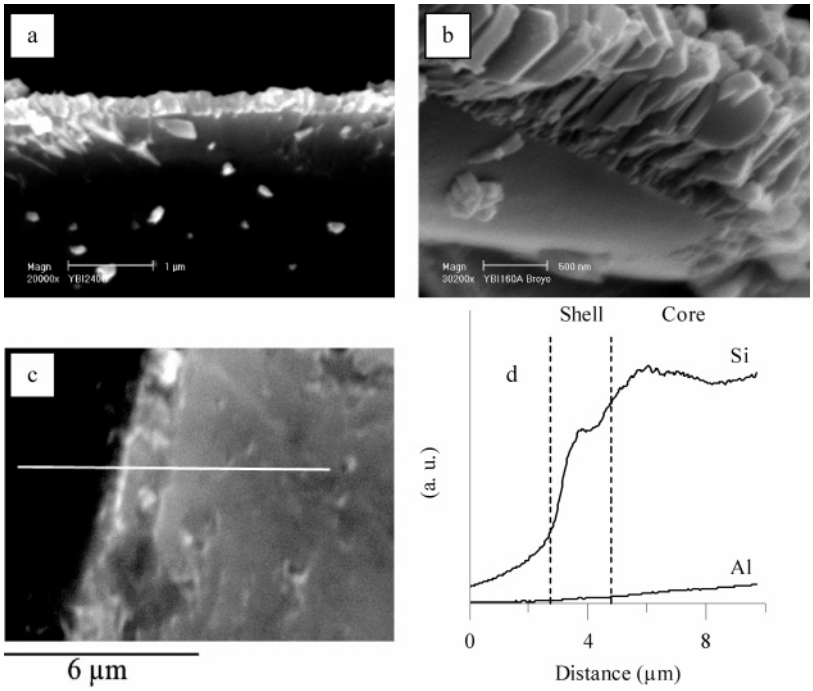

Figure 5. Silicalite-1 shells on ZSM-5 core crystals with thickness of 200 nm (a) and 800 nm (b). EDS analysis of the silicon and aluminum content in a core−shell silicalite-1−ZSM-5 composite: (c) SEM image with the profile analysis (white line) and (d) graphical presentation of the corresponding data. Dotted lines show the part corresponding to the shell.

sites on the external surface. Again, nonseeded syntheses did not provide core−shell composites although the structures of the core and shell materials are identical. Thus, the shell formation was induced by seeding as for the other couples under study.

Large ZSM-5 crystals were sufficiently stable, and the formation of core−shell composites was achieved relatively easily. The kinetics of crystal growth of the shell at 200 °C was studied, and materials with a shell thickness ranging from 200 to 1000 nm were obtained for 15 and 60 min, respectively (Figure 5a and b). Electron microprobe analysis of cross sections of core−shell composites confirmed the formation of a silicalite-1 shell. The profile lines of silicon and aluminum from the shell in inward direction are shown in Figure 5c. Besides the shell integrity, the influence of the core material on the shell composition is a question to be addressed. The chemical composition of a given zeolite is an important characteristic that defines its properties. During the crystallization process of a ZSM-5−silicalite-1 composite, the highly basic precursor mixture may react with the core and thus a partial dissolution and transport of components, namely, aluminum, from the core to the growing shell could be expected. The concentration profiles of Si and Al across the composite are shown in Figure 5d. The sodium distribution was not studied because it cannot be determined precisely by the EDS technique because of electron beam induced cation diffusion. The analysis showed trace amounts of aluminum in the shell structure and a gradual inward increase of aluminum. These data clearly show that the composition of the shell is not strongly influenced by the core material. Moreover, the EDS analysis covers a surface much larger than the shell thickness and thus is certainly influenced by the core material, which explains the presence of aluminum. Summarizing these data, one might say that if there is some dissolution and aluminum transport from the core toward the shell, it is very limited.

The silicalite-1 shell was carefully studied by TEM, and areas of different contrast were observed. The darker and lighter parts in the shell were attributed to the areas with intense and limited intergrowth, respectively (Figure 6a). The latter is most probably because of lower seed density that could not provide a well intergrown shell and often contains pinholes. A pinhole crossing almost the entire film thickness can be seen in Figure 6b. The formation of such defects could also be due to a particular orientation of intergrowing crystals as was demonstrated by Jansen et al.[27]

N_2 adsorption measurements confirmed the presence of defects in some shells. Core−shell materials synthesized for 60 min showed an S_{BET} of 120 $m^2\ g^{-1}$ which is much below that of the reference core material (400 $m^2\ g^{-1}$) but still shows the presence of uncompleted shells whose fraction was evaluated to be ca. 30%. Obviously, a second seeding−hydrothermal treatment step would have to be performed to reach close to 100% coverage.

ZSM-5 (MFI)−Zeolite Beta (BEA). The materials building the composite had a Si/Al ratio of about 14 thus providing the possibility to study the influence of this parameter on the formation of a core−shell microcomposite. Further, the combination of two microporous materials with 10- and 12-MR channel systems, respectively, may be of interest as a composite catalyst.

After the seeded synthesis, the resultant core−shell structure was subjected to XRD analysis, but evidences for the formation of zeolite Beta were not found, which is not

(27) Jansen, J. C.; van der Graaf, J. M.; van der Puil, N.; Seiger, S. B. G.; Smith, S. P. J. In *Proc. 12th Int. Zeol. Conf*., Baltimore, MD, July 5−10, 1998; Treacy, M. M J., Marcus, B. K., Bisher, M. E., Higgins, J. B., Eds.; MRS: Warrendale, 1999; Vol. I, p 603.

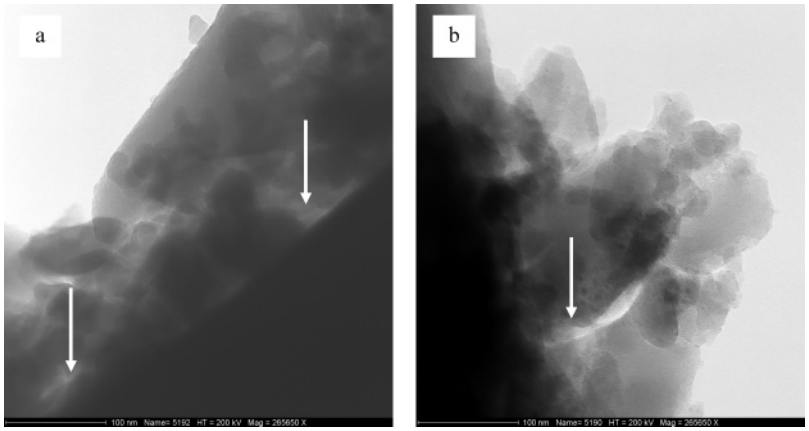

Figure 6. TEM images of a ZSM-5−silicalite-1 core−shell composite representing areas of intense (dark part) and limited (arrows) intergrowth in the shell (a) and a pinhole crossing the shell (b).

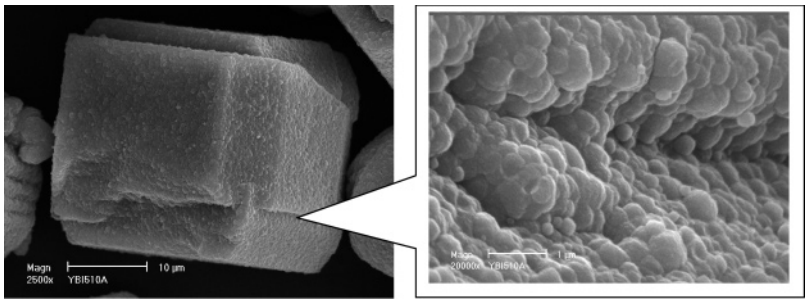

Figure 7. SEM micrographs of a ZSM-5−zeolite Beta core−shell composite. The inset represents a close view of the zeolite Beta shell at the interface between two parts of a twin crystal.

surprising having in mind that the volume fraction of the shell is negligible and that the most intense peaks of the BEA- and MFI-type framework topologies overlap. Indeed, SEM inspection showed that a polycrystalline shell was grown on the ZSM-5 twin crystals; moreover, there were not visible traces of dissolution (Figure 7). Nitrogen adsorption also showed a substantial reduction of the specific surface area, thus confirming that a large part of the calcined ZSM-5 crystals were covered by a completed TEA-Beta shell. The percentage of core crystals possessing shells impermeable to the N_2 molecule was estimated to be ca. 65%. This result is fairly similar to the one obtained for the ZSM-5−silicalite-1composite and seems to be representative for couples with compatible chemical compositions and synthesis conditions.

Discussion

The performed set of experiments showed that the formation of core−shell zeolite−zeolite microcomposites is a complex process often controlled by more than one factor. As could be expected, chemical compatibility and overlapping of crystallization fields of the core and the shell material is of great importance. These two factors are often closely related, for example, the aluminum-rich zeolites crystallize at relatively low temperature, typically around 100 °C. Further, the framework density of such materials is relatively low, for instance, for FAU- and LTA-type materials it is 13.3 and 14.2 T atoms per 1000 Å^3, respectively. On the other hand, the aluminum-poor microporous materials are generally synthesized in the temperature range 150−200 °C. Commonly, the framework density of siliceous zeolites is higher than that of the most widely used aluminum-rich zeolites (FAU- and LTA-type). Thus, differences in the chemical composition are coupled with differences in the crystallization conditions when the goal is to combine microporous materials with substantially different properties in a core−shell composite. These significant distinctions between core and shell materials were expected to be circumvented by using seeds that induce a rapid shell formation and thus protection of the core material. The series of experiments with such couples revealed, however, that the combination of such materials by in-situ growth is fairly difficult. For instance, the attempts to grow an aluminum-rich (zeolite A) shell on an all-silica core (BEA-type) crystal failed, as well as the growth of an all-silica shell (silicalite-1) on a low-silica zeolite (zeolite X). Numerous experiments with large variation of the synthesis formulations provided only materials with partial shell formation. As mentioned above, the framework composition of materials used for core and shell in these experiments was completely different. In addition, both the synthesis media and crystallization temperature did not match for these two couples.

Besides chemical considerations, there is an additional variable that deserves to be considered, namely, the framework density that is closely related with the stability of zeolitic materials. According to theoretical study performed by Foster et al.,[28] the energy factor of a zeolite structure depends on the framework density, that is, the lower the framework density the higher the energy of the structure. Consequently, microporous materials with high-energy fac-

(28) Foster, M. D.; Delgaro-Friedriches, O.; Bell, R. G.; Almeida Paz, A.; Klinowski, J. *J. Am. Chem. Soc.* **2004**, *126*, 9769.

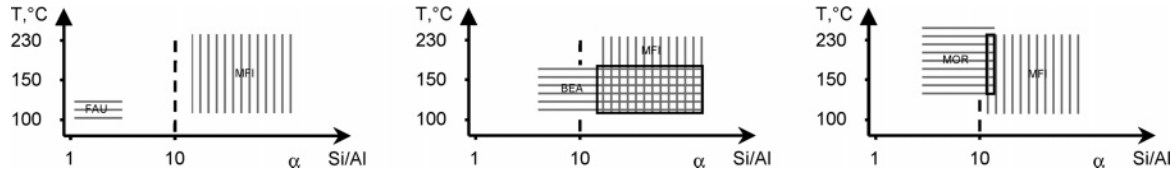

Figure 8. Diagrams combining the Si/Al ratio and crystallization temperature for the following zeolite structure types: (a) FAU−MFI, (b) MFI−BEA, and (c) MOR−MFI (adapted from ref 10b).

tors usually show low stability and could be easily transformed under hydrothermal conditions. However, the attempt to synthesis a sodalite−zeolite A composite showed that the framework density is not the key factor controlling the process. The SOD-type structure (16.7 T atoms per 1000 $Å^3$) is much denser than that of the FAU- and BEA-type materials. Nevertheless, all-silica sodalite did not show higher hydrothermal stability, and thus formation of a core−shell composite was not achieved. Hence, one may conclude that the chemical compatibility between core and shell materials and the match of crystallization conditions determine the formation of a core−shell composite. The difficulties in combining core and shell with substantially different compositions are obviously because of the dissolution of the core material within the synthesis media (Figure 3). The dissolution leads to detachment of the seeds and probably to changes in chemical equilibrium at the solution−core crystal interface. Consequently, the conditions necessary for the secondary growth of the seed crystals cannot be attended. Therefore, the secondary growth should overtake the dissolution so as to the rapid shell formation to protect the core, which is in a nonequilibrium state with the synthesis media.

The effect of chemical composition was further studied by combining zeolitic materials with very close framework composition (ZSM-5−zeolite Beta). Core−shell structures were easily synthesized which were favored by the large overlapping of the crystallization fields of these two zeolites. About 70% of ZSM-5 core crystals possessed a complete shell after one synthesis step. The rest of the crystals (ca. 30%) also possessed zeolite Beta shells. However, these shells obviously comprised pinholes and thus failed the N_2 test. As could be expected, core−shell structures comprising two MFI-type materials, namely, the aluminum-containing (ZSM-5) and the all-silica (silicalite-1) counterparts, were also successfully synthesized.

The diagrams in Figure 8 combine two important variables controlling the formation of core−shell composites, namely, the crystallization temperature and the Si/Al ratio. These diagrams clearly depict the importance of the overlapping of the composition and synthesis conditions for the successful formation of core−shell zeolite−zeolite constructs. Thus, the absence of such an overlapping between MFI- and FAU-type materials did not allow the formation of a core−shell structure (Figure 8a). This graphical presentation is also representative for the zeolite Beta (BEA)−zeolite A (LTA) couple. In contrast, the close framework compositions and synthesis conditions of zeolite Beta and ZSM-5 resulted in an easy formation of a core−shell material (Figure 8b). The pure silica forms of these two materials were also successfully combined into a core−shell structure.[10a] The formation of a MOR−MFI core−shell composite published recently[10b] reveals that at least a tiny overlapping between framework compositions and crystallization fields is necessary to synthesize a core−shell microcomposite (Figure 8c). In this case, additional factors favoring the microcomposite formation are the relatively high hydrothermal stability of mordenite and the very rapid growth of the silicalite-1 shell.

Conclusions

The possibility to synthesize core−shell zeolite−zeolite composites comprising a single-crystal core and a polycrystalline shell was studied. Preliminary seeding of core crystals and secondary growth were used to circumvent the incompatibility between the core and shell parts and to form well intergrown shells. Nevertheless, serious difficulties were observed in the preparation of certain core−shell structures. Zeolitic materials of different chemical composition were combined to study the factors controlling the formation of core−shell composites, namely, all-silica sodalite−zeolite A, zeolite Beta−zeolite A, zeolite X−silicalite-1, ZSM-5−zeolite Beta, and ZSM-5−silicalite-1. These couples offered also the opportunity to study materials crystallizing from very close to fairly different conditions.

The analysis of the results revealed that a successful formation of core−shell structures was observed for materials with compatible framework compositions and close crystallization conditions. Under close crystallization conditions, one should understand at least partial overlapping of the crystallization fields of the core and shell materials. Besides these two main factors, the rapidity of shell formation and hydrothermal stability of the core material might play an important role in the formation of a particular core−shell structure. Thus, the results of the present study may be used as guidance for possible combinations of zeolitic materials that might be prepared as core−shell composites.

The presented synthetic approach offers the possibility to synthesize core−shell composites with variable morphology since the morphology is predetermined by the core crystals. Further, the variation of the size of the core and the shell allows the control of the aspect ratio between the active part (core) and the separation part (shell), thus adapting the characteristics of the composite for any particular case. These characteristics make core−shell zeolite−zeolite composites interesting materials for many applications, ranging form the encapsulation and slow release of desired compounds to catalytic and separation processes.

Acknowledgment. The authors thank Dr. Isabel Diaz (Instituto de Catálisis Petroleoquímica, Madrid, Spain) for the TEM images, Dr. Henri Kessler (LMPC, Mulhouse, France) for helpful discussion, and partial financial support and fruitful discussion in the framework of NMP3-CT-2005-011730 IDECAT WP5.

CM0611744